BIOCHEMISTRY
including biophysical chemistry & molecular biology

ARTICLE

pubs.acs.org/biochemistry

The First Nucleotide Binding Domain of the Sulfonylurea Receptor 2A Contains Regulatory Elements and Is Folded and Functions as an Independent Module

Elvin D. de Araujo,[†] Lynn K. Ikeda,[†] Svetlana Tzvetkova,[‡] and Voula Kanelis*[,†,‡]

[†]Department of Chemistry, University of Toronto, 80 St. George Street, Toronto, Ontario M5S 3H6, Canada

[‡]Department of Chemical and Physical Sciences, University of Toronto Mississauga, 3359 Mississauga Road, Mississauga, Ontario L5L 1C6, Canada

Supporting Information

ABSTRACT: The sulfonylurea receptor 2A (SUR2A) is an ATP-binding cassette (ABC) protein that forms the regulatory subunit of ATP-sensitive potassium (K_{ATP}) channels in the heart. ATP binding and hydrolysis at the SUR2A nucleotide binding domains (NBDs) control gating of K_{ATP} channels, and mutations in the NBDs that affect ATP hydrolysis and cellular trafficking cause cardiovascular disorders. To date, there is limited information on the SUR2A NBDs and the effects of disease-causing mutations on their structure and interactions. Structural and biophysical studies of NBDs, especially from eukaryotic ABC proteins like SUR2A, have been hindered by low solubility of the isolated domains. We hypothesized that the solubility of heterologously expressed SUR2A NBDs depends on the precise definition of the domain boundaries. Putative boundaries of SUR2A NBD1 were identified by structure-based sequence alignments and subsequently tested by exploring the solubility of SUR2A NBD1 constructs with different N and C termini. We have determined boundaries of SUR2A NBD1 that allow for soluble heterologous expression of the protein, producing a folded domain with ATP binding activity. Surprisingly, our alignment and screening data indicate that SUR2A NBD1 contains two putative, previously unidentified, regulatory elements: a large insert within the β-sheet subdomain and a C-terminal extension. Our approach, which combines the use of structure-based sequence alignments and predictions of disordered regions combined with biochemical and biophysical studies, may be applied as a general method for developing suitable constructs of other NBDs of ABC proteins.

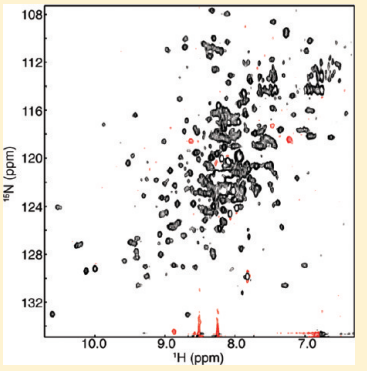

The sulfonylurea receptors, which consists of SUR1 and isoforms of SUR2, are members of the ubiquitous ATP-binding cassette (ABC) superfamily of proteins.[1] Specifically, SUR proteins are members of the C subfamily of ABC transporters (ABCC) that includes multidrug resistant proteins (MRPs) and the cystic fibrosis transmembrane conductance regulator (CFTR).[1] Like other ABC transporters, SUR proteins contain two repeats each comprised of a membrane spanning domain (MSD) followed by a cytoplasmic nucleotide binding domain (NBD). Structural data on full length transporters indicate that the transmembrane helices of the MSDs extend into the cytoplasm and are connected by short loops[2−4] and that short segments in the connecting loops, known as coupling helices, contact the NBDs.[5] The conserved structure of the NBDs includes an α/β subdomain (that contains the ATP-binding site) and the ABC-specific α-helical and β-sheet subdomains.[6] Like many ABCC proteins, such as MRP1,[1] the SUR proteins have an additional MSD that is linked to the minimum ABC structure described above by the cytoplasmic L0 linker.

Unlike most ABC proteins, the SUR proteins do not function as transporters but strictly as regulators of ATP-sensitive potassium (K_{ATP}) channels.[7] Four copies of the SUR proteins surround four copies of the pore-forming Kir6.x (Kir6.1 or Kir6.2) proteins to form K_{ATP} channels.[8] ATP binding at the Kir6.x proteins results in K_{ATP} channel inhibition whereas ATP binding and hydrolysis at the SUR NBDs results in channel opening.[9] SUR-mediated regulation of K_{ATP} channels is critical for cardiovascular and pancreatic function.[10] Over 150 different mutations that cause diseases related to insulin production have been identified in the various regions of SUR1, including in the NBDs.[11] Mutations in the NBDs of SUR2A cause dilated cardiomyopathy,[12] atrial fibrillation,[13] and increased risk of myocardial infarction.[14]

The molecular basis underlying the effects of disease-causing mutations in SUR2A on K_{ATP} channel gating are not well understood. Studies of interactions between SUR2A NBD1 and NBD2, between SUR2A NBDs and other regions of the K_{ATP} channel, or between SUR2A NBDs with other regulatory proteins require samples of the isolated SUR2A NBDs. However, attempts at heterologous expression of the NBDs of eukaryotic ABC transporters, including SUR1 and SUR2A, as isolated

Received: March 23, 2011
Revised: June 28, 2011
Published: June 29, 2011

proteins has been challenging with the majority of eukaryotic NBDs expressed as inclusion bodies in *E. coli*.[15,16] In some cases, the protein has been refolded.[17,18] However, *in vitro* refolding of multidomain proteins like the NBDs is difficult and oftentimes results in a heterogeneous population of refolded protein. Thus, strategies for heterologous expression of eukaryotic NBDs in *E. coli* in a soluble form need to be investigated and may include altering cell type and choosing expression vectors under the control of different promoters. For example, the successful expression and isolation of soluble NBD1 from P-glycoprotein required the use of pBAD-derived plasmids in which protein expression is under the control of the araBAD promoter, rather than pET-based expression plasmids that control protein synthesis via the *lac* operon.[19] Other strategies for obtaining soluble NBDs from eukaryotic ABC transporters include fusing the NBD with carrier proteins such as maltose binding protein (MBP), glutathione S transferase (GST), or thioredoxin.[17,20,21] Some of these tags, specifically GST, form dimers and higher order oligomers and must be removed prior to biochemical and structural studies, often resulting in limited solubility of the isolated NBD.

The identification of correct domain boundaries is critical to the heterologous expression of NBDs in a soluble form in *E. coli*. Ideally, domain boundaries should be chosen so as to not eliminate any structured regions of a globular domain, which would prevent proper folding and lead to aggregation. Further, flexible regions N- and C-terminal to the structured domain should be excluded as they often reduce solubility. Determination of correct boundaries for NBDs is complicated by the relatively low sequence identity between NBDs outside the conserved residues involved in ATP binding and hydrolysis. In this paper, we have investigated the domain boundaries of the first nucleotide binding domain (NBD1) from SUR2A. We hypothesize that the identification of correct N- and C-terminal boundaries is necessary for production of soluble SUR2A NBD1 in *E. coli* cells. In addition, the use of correct boundaries should enable removal of the fusion partner without compromising solubility of the isolated domain. We have used a combination of structure-based sequence alignments and predictions of disordered regions to identify potential domain boundaries for SUR2A NBD1. We have tested a variety of different domain boundaries on protein expression and solubility. Our screen of these different constructs identified boundaries (S615-L933) necessary for the production of isolated SUR2A NBD1 in a soluble form at high concentrations. Circular dichroism (CD) and nuclear magnetic resonance (NMR) spectroscopy indicate that SUR2A NBD1 S615-L933 is folded, and ATP binding studies demonstrate that the protein has ATP binding activity. Surprisingly, our alignment demonstrates the presence of a large insert between the first two β-strands of the β-sheet subdomain in SUR2A NBD1 that must be considered when defining the N-terminal domain boundary. Further, our experiments provide evidence that residues C-terminal to the canonical structured domain aid in stability. Comparison with the NBD1 of CFTR, another ABCC protein, suggests regulatory roles for the β-sheet subdomain and C-terminal extension of SUR2A NBD1. Our method, which combines the use of structure-based sequence alignments and predictions of disordered regions with biochemical and biophysical studies, may be applied as a general approach for developing suitable constructs of NBDs from other ABC proteins.

EXPERIMENTAL PROCEDURES

Structure-Based Sequence Alignment of the SUR NBDs. In order to determine the N-terminal and C-terminal boundaries of the SUR NBDs, a structure-based sequence alignment was generated with ClustalW.[22,23] Our alignment included the NBDs from all currently identified mammalian C subfamily ABC transporters (ABCC),[1] NBDs from the yeast ABCC protein Ycf1p, and NBDs from other ABC proteins for which the structure has been solved.[2,6] Secondary structure data from the crystal structures of NBD1 from CFTR,[16,24] an ABCC protein, and the NBD from the TAP1 transporter[25] were used to generate the structure-based sequence alignment. The penalty for introducing gaps in α-helices and β-strands was set to the highest value (equal to 9 from a possible range of 0−9), while the gap penalty for unstructured regions was set to a low value of 2.[22] These settings allow for gaps and insertions in unstructured loops and termini and not in secondary structural elements.

Expression and purification of different SUR2A NBD1 constructs. Rat SUR2A NBD1 proteins containing different N- and C-terminal boundaries (Figure 1) were expressed as N-terminal-6xHis-SUMO fusion proteins[26] using a pET26b-derived expression vector.[16] Different N- and C-termini were chosen to test the effects of removing putative secondary structural elements on protein stability and solubility. Proteins were expressed in *E. coli* BL21 (DE3) CodonPlus-RIL (Stratagene) grown either in LB media or M9 minimal media with isotopic enrichment for NMR spectroscopy as necessary. Cells were grown at 37 °C until an OD600 of 0.8, at which point the incubating temperature was reduced to 16 °C and gene expression was induced with 0.75 mM isopropyl β-D-thiogalactoside (IPTG). After 16 h, cells were harvested by centrifugation and pellets were stored at −20 °C. Protein expression was induced at 16 °C, as lower temperature induction has been previously shown to yield more soluble protein compared with expression at 37 °C, including SUR2A NBD1 (data not shown).

Protein purification was conducted at 4 °C. All six constructs were purified using the same procedure, which is very similar to that used for purification of NBD1 from CFTR.[16] Cell pellets were resuspended in lysis buffer (50 mM tris pH 7.6, 100 mM arginine, 150 mM NaCl, 2 mM β-mercaptoethanol, 2 mM ATP, 5 mM $MgCl_2$, 12.5% (v/v) glycerol, 0.2% (v/v) Triton X-100, 2 mg/mL deoxycholic acid, 1 mg/mL lysozyme, 5 mM 6-aminocaproic acid, 5 mM *p*-aminobenzamidine, and 1 mM PMSF). Cells were resuspended in 10 mL of lysis buffer per unit OD_{600} per L of culture. Cells were lysed by sonication and centrifuged to remove cell debris. The 6x-His-SUMO-NBD1 was loaded onto a High Performance Ni^{2+}-NTA affinity column (GE Healthcare) in equilibration buffer containing 20 mM tris pH 7.6, 500 mM NaCl, 5 mM imidazole, 12.5% (v/v) glycerol. The column was washed with 10 column volumes of equilibration buffer, and the protein was eluted in 20 mM tris pH 7.6, 150 mM NaCl, 500 mM imidazole, 12.5% (v/v) glycerol, 2 mM ATP, 5 mM $MgCl_2$, 2 mM β-mercaptoethanol. Eluents containing the protein were pooled and diluted with gel filtration buffer (20 mM tris pH 7.6, 500 mM NaCl, 12.5% (v/v) glycerol, 2 mM ATP, 5 mM $MgCl_2$, 2 mM β-mercaptoethanol) so that the final imidazole concentration was ≤200 mM. The 6x-His-SUMO tag was cleaved from NBD1 with a His-tagged Ulp1 protease. The resultant mixture was concentrated using a centrifugal filter (Millipore) and loaded onto a 24 mL Superdex 75 gel filtration column (GE Healthcare) pre-equilibrated with gel filtration buffer. The fractions containing NBD1 were collected and applied to a Ni^{2+}-NTA affinity column (GE Healthcare) to remove both the His-tagged Ulp1 protease and contaminating amounts of 6x-His-SUMO from NBD1. The presence of NBD1 was confirmed by SDS-PAGE

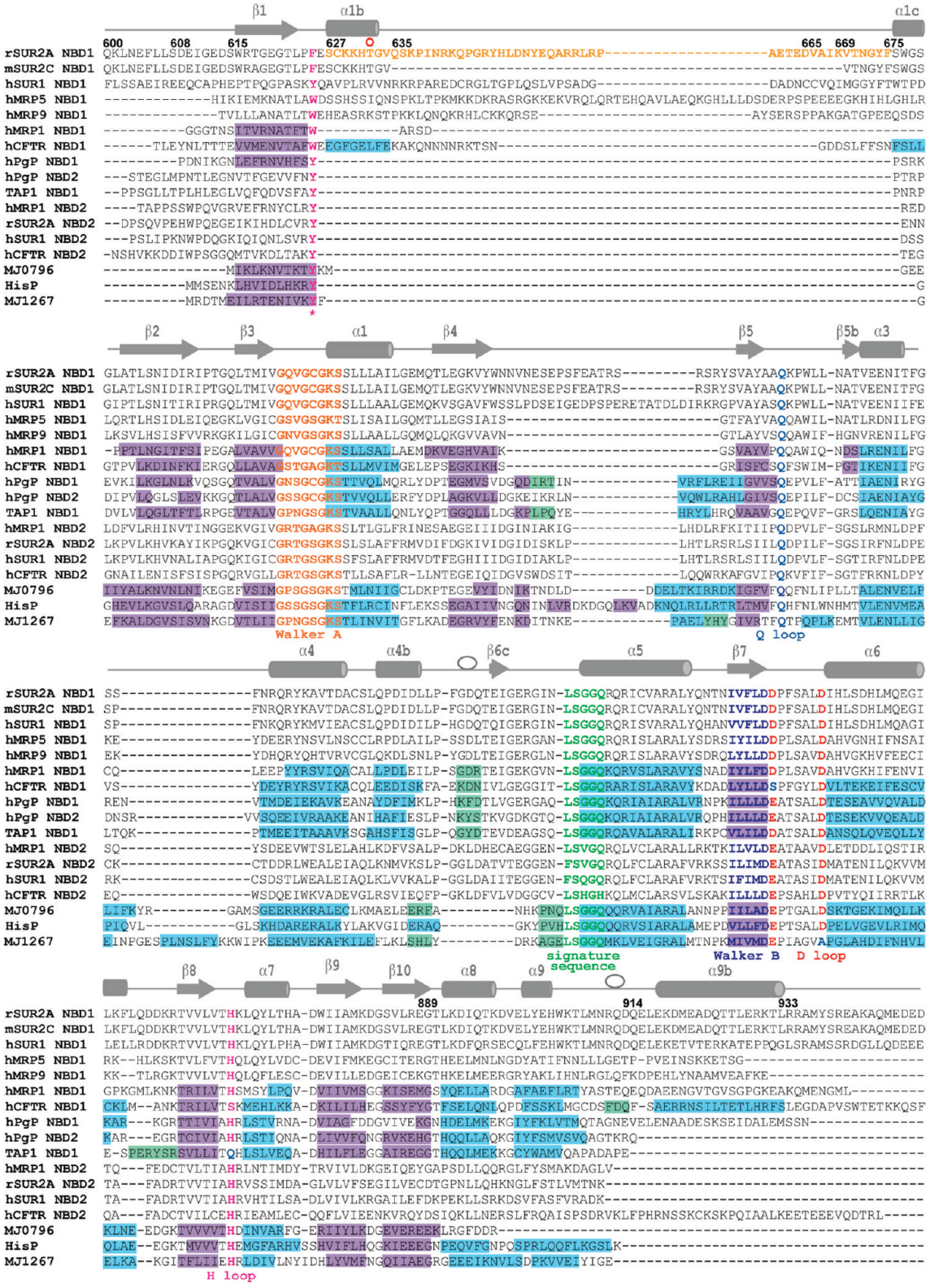

Figure 1. Selected sequences from the structure-based sequence alignment of ABC NBDs. The secondary structure of NBD1 from human CFTR NBD1 (ref 24 and PDB code 1XMI) is displayed above the alignment in gray, with α-helices represented as cylinders, β-sheets as arrows, and 3_{10}-helices as open circles. Secondary structure elements in known structures are highlighted in purple for β-strands, blue for α-helices, and green for 3_{10}-helices. Conserved residues in the Walker A and Walker B motifs, signature sequence, and Q, D, and H loops are in bold, with the motif labeled below the alignment. An asterisk (∗) highlights a conserved aromatic C-terminal to the β1 strand, which is involved in binding the adenine ring of ATP. Residues comprising the β-sheet subdomain insert in SUR2A NBD1 are highlighted in light orange. The PKA phosphorylation site, T632, in rSUR2A and mSUR2C is indicated by a red open circle above the alignment. Residue numbers referred to in the text are shown above the sequence.

dx.doi.org/10.1021/bi200434d |*Biochemistry* 2011, 50, 6655–6666

and protein concentration was determined via amino acid analysis.

For NMR studies, the purified NBD1 protein was dialyzed into NMR buffer containing 20 mM Na phosphate, pH 7.2, 150 mM NaCl, 5 mM $MgCl_2$, 2 mM ATP, and 2% (v/v) glycerol.

Circular Dichroism Spectroscopy. Circular dichroism (CD) spectra of purified SUR2A NBD1 were recorded from 200 to 300 nm at 22 °C on an Aviv 250 CD spectrometer (Aviv Biomedical Inc., Lakeview, NJ) with a bandwidth of 0.2 nm using a 1 cm path length quartz cell. Samples contained 5 μM NBD1 in 20 mM phosphate, pH 7.25. Spectra were averaged from three scans and baseline-corrected by using a blank consisting of buffer only.

NMR Spectroscopy. TROSY-HSQC spectra[27,28] were recorded at 30 °C on a 600 MHz Varian Inova spectrometer equipped with a H(F)CN triple resonance cryoprobe and actively shielded *z*-gradients. The NBD1 concentration was 0.1−0.5 mM. Data were processed using NMRPipe/NMRDraw[29] and analyzed using NMRView.[30]

Homology Modeling of NBD1. Homology models of rat SUR2A NBD1 were generated based on the structure-based sequence alignment using the program Modeller.[31] The crystal structure of NBD1 from CFTR was used as templates (ref 24 and PDB code 1XMI). A total of 50 models were generated from which the 10 lowest energy models were selected for analysis. Homology models were evaluated by ProSA[32,33] to assess the model fold and PROCHECK[34] to assess the stereochemistry of the models.

ATPase Assays. The ATPase activity of rSUR2A NBD1 (S615-L933) was determined with the ENZChek Phosphate Assay Kit (Molecular Probes), which uses a spectrophotometric method to measure the amount of inorganic phosphate (P*i*) in solution. In summary, purine nucleoside phosphorylase converts 2-amino-6-mercapto-7-methylpurine riboside (MESG), which has a maximum absorbance at 330 nm, to ribose 1-phosphate and 2-amino-6-mercapto-7-methylpurine, which has a maximum absorbance at 360 nm. The reaction requires 1 equiv of P*i*, and thus, the method can be used to measure the activity of ATPases, such as the SUR NBDs, by coupling the two enzymic reactions.[35]

Solutions of MESG, purine nucleoside phosphorylase, and the phosphate standard were prepared according to the manufacturer's instructions. ATP stocks (100 mM) were prepared fresh in 50 mM Tris HCl, pH 7.5, 1 mM $MgCl_2$. ATP was removed from preparations of SUR2A NBD1 by size exclusion chromatography. Reaction samples consisted of 2 mM ATP, 0.1 mg of SUR2A NBD1, 0.2 mM MESG, and 1 U of purine nucleoside phosphorylase in a total volume of 1 mL. Blank reactions lacking protein were also prepared to assess any background P*i* and spontaneous ATP hydrolysis. Reaction and blank samples were incubated at 37 °C for 30 min, at which point the A_{360} was measured using an Ultrospec 2100 pro spectrophotometer.

RESULTS

Determination of SUR2A NBD1 Boundaries. N- and C-terminal boundaries of rat SUR2A (rSUR2A) NBD1 were predicted from a structure-based sequence alignment of all NBDs from the ABCC family of proteins as well as NBDs from other proteins for which the structures have been solved (Figure 1 and Supporting Information Figure 1). The secondary structure masks used in the alignment were the crystal structures of CFTR NBD1[16,24] and TAP1 NBD1.[25] CFTR is another ABCC protein and, hence, a good model for NBD1s from other ABCC family members. Our alignment shows excellent agreement in the position of conserved residues involved in nucleotide binding and hydrolysis. Although secondary structure masks were used only from the NBD1s of CFTR[16,24] and TAP1,[25] there is excellent agreement among secondary structures of all NBDs in our final alignment. The high quality of our alignment is also demonstrated by the alignment of a conserved aromatic residue immediately C-terminal to the first β-strand (β1), even though there is little sequence identity between NBDs in this region. This aromatic residue is involved in stacking interactions with the adenine ring in all known structures of ATP-bound NBDs.[36]

Interestingly, our alignment predicted a previously unreported insert (S627-F675) in SUR2A NBD1 between the first two strands of the β-sheet subdomain that is not observed in most NBDs, including bacterial NBDs, NBD1 and NBD2 from P-glycoprotein, and NBD2s from ABCC proteins. This insert is present in all of the alignments that we have performed, regardless of whether or not secondary structure masks were employed (data not shown), with the use of secondary structure masks resulting in better definitions for the N- and C-terminal ends of the inset. A similar β-sheet subdomain inset was originally seen in the crystal structure of CFTR NBD1.[16,24] Known as the regulatory insert (RI) in CFTR NBD1, this insert was thought to be unique to CFTR.[16] However, our alignment indicates that many of the NBD1s in the ABCC subfamily, in addition to CFTR and SUR NBD1s, possess such an insert. Structural data on CFTR NBD1 indicate that the RI is formed by two α-helices (referred to as helices α1b and α1c) separated by a disordered loop.[16,24] Lack of sequence conservation in this region precludes identification of similar secondary structures (i.e., α1b and α1c helices) in the β-sheet subdomain inserts of other ABCC proteins, including SUR2A. Notably, a naturally occurring splice isoform of SUR2 that lacks exon 14, which corresponds to residues Q635-K669 in rat SUR2A,[37] and is known as SUR2C (Figure 1) is missing much of this insert.

The sequence of SUR2A was subjected to the neural network program PONDR.[38−40] The VLXT algorithm, which is currently the most accurate algorithm for predicting disorder, predicts that many of the residues encoded by exon 14 (Q635-E664) are disordered (Supporting Information Figure 2). Of note, residues Q635-K669 align with the disordered loop in the RI of CFTR NBD1 (Figure 1), perhaps suggesting that the β-sheet subdomain insert in SUR2A has a function similar to that of the RI in CFTR.

An important consequence of such a large insert after the first β-strand in SUR2A NBD1 is that the beginning of the domain is ∼50 residues N-terminal of where originally thought.[41,42] Using our alignment, we predict that the N-terminal boundary of SUR2A NBD1 is between Q600 and T618 and thus chose N-terminal boundaries of Q600, S608, S615, and T618 for our constructs. Alignment data predicted that the C-terminal boundary was at either D914 or L933. From our alignment, D914 is located just C-terminal to α-helix α9, the last structured element in most NBDs,[6] whereas L933 extends beyond the canonical structured regions seen in most NBDs. However, there is sequence similarity in this region between the SUR NBDs and NBDs from other ABCC subfamily members, particularly NBD1 from CFTR. CFTR NBD1 residues that align with SUR2A NBD1 residues Q915-L933 adopt an α-helical structure (helix α9b)[16,24] and form the regulatory extension (RE) in CFTR. X-ray[16] and NMR data[43,44] of CFTR NBD1 indicate that the RE

Table 1. Expression, Purification, and Characterization of SUR2A NBD1 Constructs

domain boundaries	overexpression	total yield (mg/L)	max protein concen[a] (μM)	notes
Q600-L933	yes	N.D.[b]	N.D.[b]	insoluble
S608-L933	yes	80	>500	soluble and folded (CD); aggregation at high concentrations (NMR)
S615-L933	yes	60, 10 (M9)[c]	~500	soluble and folded (NMR and CD)
S615-D914	yes	3	<50	very low solubility
T618-L933	yes	6 (M9)[c]	300	soluble and folded (NMR)
D665-E889	very poor	N.D.[b]	N.D.[b]	insoluble

[a] Concentrations reported are for isolated domain in the NMR buffer. [b] N.D.: could not be determined due to lack of soluble protein. [c] Expression was performed in M9 minimal media. For all other samples, expression was done in LB.

(and RI) are involved in dynamic interactions with the NBD1 core. This prompted us to investigate the effect of two different C-terminal boundaries, D914 and L933.

We also tested a much smaller construct from D665-E889,[41,42] which according to our alignment removes the N-terminal β-strand (β1) and ends before the α-helix α8. However, sequence analysis by the PONDR algorithm VSL1[45] indicates that residues E610 to T663 are disordered, suggesting that the first residue of the structured region of NBD1 may be C-terminal to T663.[41] The C-terminal boundary excludes helix α8 as seen the bacterial NBD MJ0976.[46] Work done on this construct indicates that some soluble, isolated NBD1 can be obtained for biophysical studies, although at very low concentrations.[42]

In order to test the quality of our sequence alignment, homology models of SUR2A NBD1 (residues Q600-L933) were generated with Modeller using the crystal structure of human CFTR NBD1 (ref 24 and PDB code 1XMI) as the template (Supporting Information Figure 3). A total of 50 structures were generated, of which the 10 lowest energy models were chosen for analysis. All SUR2A NBD1 homology models have the canonical structure seen in other NBDs, consisting of the β-sheet subdomain, the α/β subdomain that binds ATP, and α-helical subdomain. The two α-helices present in the β-sheet subdomain insert located between strands β1 and β2 are seen only in structures of CFTR NBD1 and hence may be reflective of the CFTR NBD1 template used and may not be present in SUR2A NBD1 or NBDs from other ABC transporters. All 10 lowest energy models have ProSA Z scores and residue energies that are within the range for experimentally determined structures of similar size.[32,33] The 10 lowest energy models also have good stereochemistry as evaluated by PROCHECK.[34] Together, these results indicate our homology models, and by extension our structure-based sequence alignment, are of good quality.

Expression, Purification, and Solubility of SUR2A NBD1 Constructs. The domain boundaries determined from our structure-based sequence alignment were applied to studies of NBD1 from rat SUR2A, which has only 12 single amino acid substitutions and one amino acid deletion compared to human SUR2A NBD1. We opted to express rat SUR2A NBD1 proteins as fusions with yeast SUMO, as this fusion partner enhances soluble expression of proteins in *E. coli*,[47] including CFTR NBD1.[16] A total of six constructs of rat SUR2A NBD1 were designed to verify the domain boundaries obtained from the alignment and to test the effect of variable structured regions (i.e., at the C terminus) on the stability and solubility of the domain. Our screening of domain boundaries was based on a number of criteria. First, choosing correct boundaries would result in folded, stable NBDs that are solubly expressed in *E. coli*, as proteins that are not folded correctly are often expressed in inclusion bodies. Further, nonaggregated protein could be cleaved from the His-SUMO fusion.[16] Recognition of the C terminus of SUMO by the Ulp1 protease requires that the SUMO is correctly folded, but also that the fusion partner is not aggregated in solution, which would likely cause limited access of the substrate to the Ulp1 protease. Our final criterion for choosing correct domain boundaries was that the isolated NBD would not aggregate and, therefore, could be concentrated to the high concentrations (0.1−0.5 mM) required for characterization by NMR spectroscopy. The results of the heterologous expression in *E. coli*, solubility, and structural characterization of the SUR2A NBD1 constructs are described below and summarized in Table 1.

Expression levels for the 6xHis-SUMO NBD1 fusion proteins fall into two main categories (Supporting Information Figure 4A). High levels of overexpression were achieved for constructs that contained all essential secondary structure elements, which included Q600-L933, S608-L933, S615-L933, and S615-D914. The T618-L933 construct, which is missing the first two residues of the β-strand β1, also had high levels of overexpression, but not as high as constructs that started at S615, S608, or Q600. In contrast, there is no evidence of overexpression of the D665-E889 construct, similar to other observations.[41,42] Of note, in SDS-PAGE the Q600-L933 fusion protein migrates at a molecular mass lower than expected. The apparent lower molecular mass for the Q600-L933 fusion protein may be due to protein instability in the cell, resulting in proteolysis, or an altered conformation in the SDS-PAGE compared to the other fusion proteins. Most of the fusion proteins also have significant levels of soluble expression in LB media (Supporting Information Figure 4B). Because of the low level of expression, it is difficult to ascertain how much soluble protein is produced with the D665-E889 construct. The D665-E889 construct could only be detected in the Ni^{2+} purification of the protein.

The 6xHis-SUMO NBD1 fusion proteins in the soluble fractions were initially purified using Ni^{2+} affinity chromatography, as shown for S615-L933 in Figure 2A. The 6x-His-SUMO tag could be removed for all of the constructs by incubation with Ulp1 protease, which recognizes the C terminus of SUMO (Figure 2B). However, removal of the tag for Q600-L933 and D665-E889 resulted in precipitation of most of the protein, precluding further purification of these two constructs.

After digestion with Ulp1 protease, S608-L933, S615-L933, S615-D914, and T618-L933 were further purified by size exclusion chromatography (Figures 2C,D and 3). The majority of each NBD1 construct (~36 kDa) elutes at ~10.7 mL, which is an elution volume that is slightly larger than the elution volume of 11.0 mL for a 44 kDa standard protein. The earlier elution

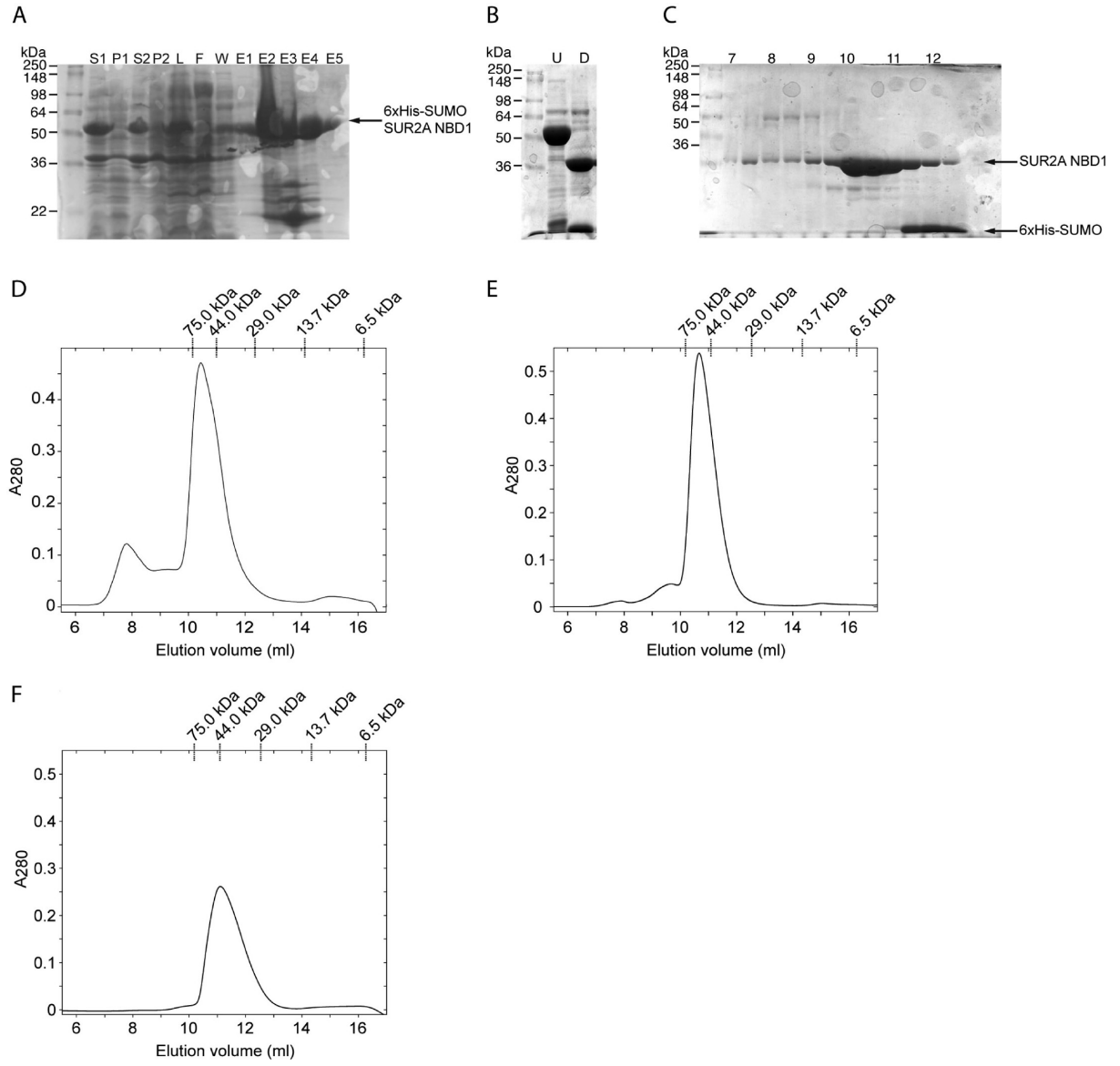

Figure 2. Purification of SUR2A NBD1 (S615-L933). (A) Ni^{2+} affinity chromatography of 6xHis-SUMO SUR2A NBD1 (S615-L933) as described in the Experimental Procedures section. In each case, the amount of sample loaded corresponded to 1/500 of the total volume of the fraction. Lanes show the soluble (S1 and S2) and insoluble fractions (P1 and P2) from two different sonications, supernatant after lysing the cells (L), proteins that did not bind the Ni^{2+} column (F), wash fractions (W), and the five mL elution fractions (E1−E5). (B) Ulp1 digestion of 6xHis-SUMO SUR2A NBD1 showing undigested (U) and digested (D) samples. (C) Gel filtration purification of SUR2A NBD1 with elution volume indicated above each lane (see panel D). from repeat runs on the gel filtration column. (D) A_{280} trace from gel filtration purification of SUR2A NBD1 (S615-L933). (E) A_{280} trace from gel filtration analysis of purified SUR2A NBD1 S615-L933. The sample was applied and run in the NMR buffer with 5% (v/v) glycerol, rather than 2%. (F) A_{280} trace from gel filtration analysis of purified SUR2A NBD1 S615-D914 of ~0.2 mM. The sample applied to the gel filtration column contained 12.5% (v/v) glycerol, and the running buffer was the NMR buffer with 2% (v/v) glycerol. Note: we cannot concentrate SUR2A NBD1 S615-D914 to 0.5 mM, as for S615-L933, even with high concentrations of glycerol. Hence the absorbance of the gel filtration analysis of SUR2A NBD1 S615-D914 is lower than that observed for SUR2A NBD1 S615-L933 in panel E. The elution volumes of molecular weight standard proteins (GE Healthcare) are indicated at the top of each trace in panels D−F. The difference in elution profiles of the standards between panels D and E and F are due to different buffer conditions (gel filtration buffer for panel D with 12.5% (v/v) glycerol, NMR buffer for panel E with 5% (v/v) glycerol, and NMR buffer for panel F with 2% (v/v) glycerol) and flow rates (0.3 mL/min for panel D and 0.5 mL/min for panels E and F).

volume of NBD1 is likely due to the presence of the large disordered β-sheet subdomain insert of 49 residues and the C-terminal extension (Q915-L933), which is also predicted to be disordered by PONDR (Supporting Information Figure 2). The presence of significant disordered residues in NBD1 (68 disordered residues of 319 total) is expected to significantly increase the hydrodynamic radius of NBD1, thus resulting in an earlier elution profile of NBD1 compared to a globular protein of 36 kDa.[48] Consistent with this hypothesis, removal of the C-terminal extension (S615-D914) results in elution of a peak at 11.0 mL (Figure 2F). The earlier than expected elution of S615-L933 is unlikely due to protein aggregation, as application of samples with higher and lower concentrations of protein results in the same elution profile (data not shown). In each case,

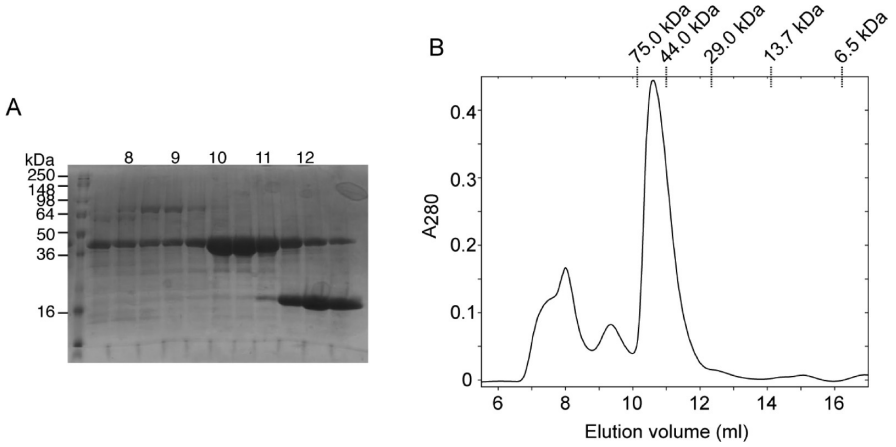

Figure 3. Size exclusion purification of SUR2A NBD1 (S608-L933). (A) Gel filtration purification of SUR2A NBD1 showing pooled eluents from repeat runs on the gel filtration column with the elution volume indicated above each lane (see panel B). (B) A_{280} trace from gel filtration purification of SUR2A NBD1. The elution volumes of molecular weight standard proteins (GE Healthcare) are indicated at the top of the trace. Notice the increase in species eluting at higher molecular weight compared with S615-L933. The conditions (buffer and flow rate) for gel filtration purification of SUR2A NBD1 S608-L933 are identical to that of SUR2A NBD1 S615-L933 (Figure 2D).

a small amount of protein coelutes with a higher molecular weight contaminant, similar to size exclusion data for other NBDs.[19] This behavior is most pronounced for S608-L933 (Figure 3), but also apparent in S615-L933 (Figure 2), and may be due to nonspecific interactions between SUR2A NBD1 and endogenous *E. coli* proteins at the high protein concentrations applied to the size exclusion column or due to protein aggregation. Of note, application of a 0.60 mM sample of purified SUR2A NBD1 S615-L933 to the size exclusion column in the NMR buffer results in one main peak at ~10.7 mL (Figure 2E), indicating that formation of nonspecific interactions does not affect the elution profile of SUR2A NBD1 during purification. We interpret the smaller peak at 9.5 mL to be caused by conformational changes in SUR2A NBD1 (S615-L933) that alter the shape of the protein significantly so that the elution profile contains more than one peak, reflecting more than one population of molecules. One possible cause of such conformational changes may be the presence of the C-terminal extension (and β-sheet subdomain insert), as elution profiles of purified SUR2A NBD1 lacking this region (from S615-D914) do not possess an elution peak at 9.5 mL (Figure 2F). Of note, our NMR spectra of SUR2A NBD1 S615-L933 are suggestive of conformational dynamics (see below).

A significant difference between the behavior of the different NBD1 constructs is the total yield of soluble protein once the fusion tag is removed. Constructs S608-L933 and S615-L933 yield 80 and 60 mg of purified protein per liter of LB culture, respectively. Construct T618-L933 yields 6 mg of purified protein per liter of M9 culture compared with 10 mg per liter of M9 media for S615-L933. Much less purified protein was obtained for SUR2A NBD1 S615-L914 (3 mg per liter of LB culture), mainly because most of the protein precipitates once the 6xHis-SUMO fusion tag is removed. Further, the SUR2A NBD1 S608-L933, S615-L933, and T618-L933 proteins could be concentrated to ~0.3−0.5 mM in the presence of MgATP and with low (2%, v/v) concentrations of glycerol, as required for NMR studies. Such high concentrations were not possible for the S615-D914, which could only be concentrated to ~20 μM before precipitation occurred. The construct S615-D914 is missing residues Q915-L933 that correspond to the RE in CFTR NBD1. The low *in vitro* solubility of S615-D914 compared to S615-L933 shows that residues Q915-L933 impart stability to SUR2A NBD1. Thus, we focused additional studies on SUR2A NBD1 constructs ending with residue L933.

Structural Characterization. The different SUR2A NBD1 constructs that are soluble to 200−500 μM (S608-L933, S615-L933, T618-L933) were characterized by NMR spectroscopy. The 2D ^{15}N−^{1}H TROSY-HSQC spectrum of a 320 μM sample SUR2A NBD1 S615-L933 in the presence of Mg/ATP is shown in Figure 4A. The dispersion of resonances in the ^{1}H dimension, from ~6.5 to ~9.5 ppm for backbone H^N resonances, demonstrates that SUR2A NBD1 S615-L933 is folded. Of note, the NMR resonances of SUR2A NBD1 have different intensities (Figure 4B). Some resonances are very sharp, while other resonances have broad, weak signals. The sharp resonances, centered at ~8.2 ppm in the ^{1}H dimension, are characteristic of disordered regions, which may include the large β-sheet subdomain insert and the C-terminal extension. The significant broadening for some resonances is likely caused by motion on the microsecond−millisecond time scale, suggesting significant protein dynamics for SUR2A NBD1. To ensure that the broadening was not caused by dimerization of NBD1 at concentrations >300 μM used in our NMR experiment, we also recorded TROSY-HSQC spectra on a sample of SUR2A NBD1 (S615-L933) taken directly from the eluent (at 10.7 mL) of the size exclusion column (Figure 2E) without concentrating the sample further. The final concentration of the NMR sample using protein in this fraction was 50 μM. Identical spectra, in peak positions and relative peak intensities, were obtained of SUR2A NBD1 at 50 μM (Figure 4C), indicating that there is no concentration-dependent aggregation or change in oligomeric state (i.e., dimerization) under these conditions. The absence of dimerization of SUR2A NBD1 in the presence of ATP is consistent with observations of other NBDs from eukaryotic ABC transporters, in which NBD1 and NBD2 are not identical, that demonstrate monomeric behavior of NBD1 even at the high concentrations used in structural studies.[16,24,44,49] Our high quality TROSY-HSQC NMR spectra indicate that detailed studies, including resonance assignments, of the isolated SUR2A NBD1 (S615-L933) and protein complexes are feasible.

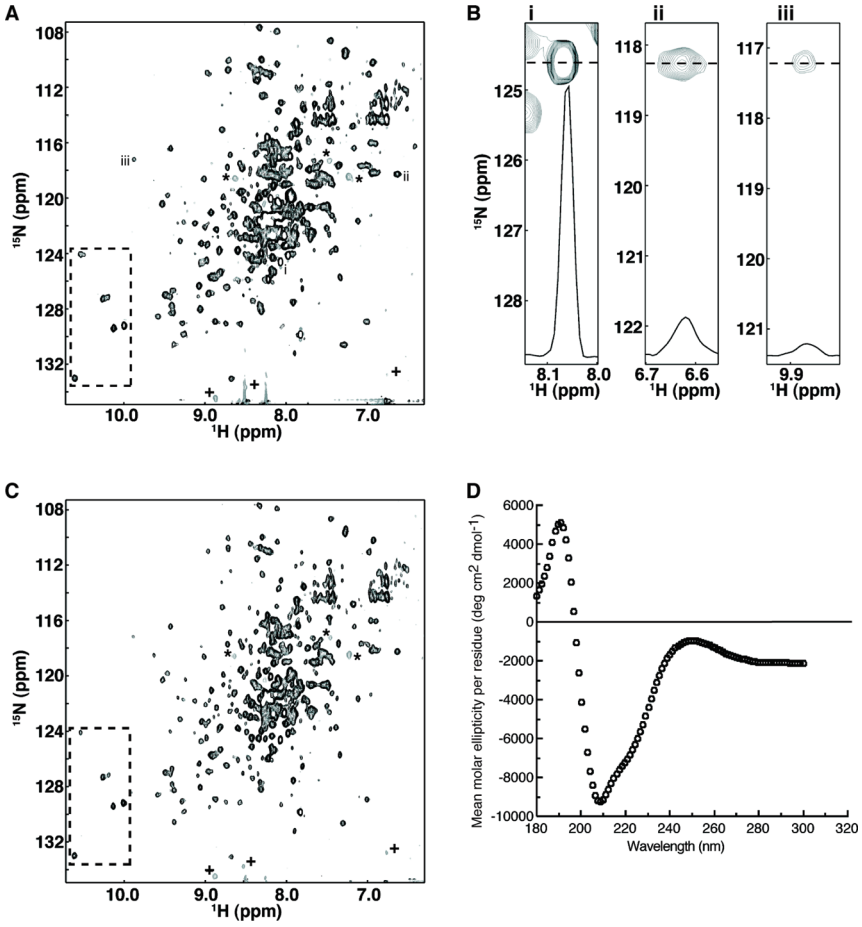

Figure 4. Structural characterization of SUR2A NBD1 S615-L933. (A) 2D ^{15}N−^{1}H TROSY-HSQC[27] spectrum of SUR2A NBD1 (0.32 mM) with 5 mM Mg^{2+} and 5 mM ATP in 20 mM Na phosphate, pH 7, 150 mM NaCl, 2% (v/v) glycerol, 5 mM DTT, 10% (v/v) D_2O at 30 °C at 600 MHz. Chemical shifts were referenced to 4,4-dimethyl-4-silapentane-1-sulfonic acid (DSS). Resonances of backbone nuclei, as well as those from side chain nuclei from Trp, Asn, and Gln residues, are shown in black. The black resonances enclosed in the dashed box are from side chain Trp indole HN. There are six Trp residues in the protein and six resolved resonances in the dashed box. The gray resonances are of opposite sign, caused by spectral aliasing, and are possibly from Arg NεHε side chain correlations (marked with an "∗") or backbone NH correlations from Gly residues (marked with a "+"). (B) Selected regions of the spectra showing peaks of markedly different intensities. A trace through the approximate center of the peak is shown at the bottom of each spectrum, illustrating the line shape. Three different resonances were chosen, identified as (i), (ii), and (iii) in panel A. Very intense resonances in the center of the spectra, such as the peak represented by (i), may arise from disordered loops in NBD1, including the loop encoded by exon 14. Very weak resonances, such as the peak represented by (iii) are due to conformational exchange in the protein. (C) 2D ^{15}N−^{1}H TROSY-HSQC[27] spectrum of 50 μM SUR2A NBD1 in solution conditions identical to those used to record the spectrum in panel A. (D) Circular dichroism spectrum of SUR2A NBD1. Far-UV CD spectra were obtained in a 0.1 cm path length cuvette at 22 °C. The sample concentration was 5 μM protein in 20 mM phosphate pH 7.25. The mean residue ellipticity is plotted as a function of wavelength and represents the average of three scans. The CD spectra of SUR2A NBD1 S615-L933 is consistent of a folded protein with mixed α-helix/β-sheet secondary structure.

TROSY-HSQC spectra were also recorded for SUR2A NBD1 S608-L933 (500 μM) and SUR2A NBD1 T618-L933 (300 μM). While spectra of the T618-L933 construct are of high quality and similar to spectra of SUR2A NBD1 S615-L933, spectra of the S608-L933 construct are of much poorer quality (data not shown). Only few very intense resonances centered at ∼8.2 ppm in the ^{1}H dimension are visible, while other weaker resonances are broadened significantly. The spectra and behavior of S608-L933 on the gel filtration column (Figure 4A) suggest that the protein forms low molecular weight aggregates in solution. The higher concentration of protein in the S608-L933 sample (500 μM) versus the S615-L933 sample (320 μM) is unlikely the cause of this aggregation because a comparison of spectra of 500 μM samples of SUR2A NBD1 S615-L933 and S608-L933 at 25 °C also indicates aggregation of S608-L933 but not S615-L933 (data not shown). Because of the high quality of the NMR spectra, yield, and solution properties of SUR2A NBD1 S615-L933, we decided to focus our additional studies on this construct. CD spectroscopy was used to characterize the secondary structure of S615-L933 (Figure 4D). As expected, the CD spectrum of the S615-L933 NBD1 is characteristic of a folded protein with mixed α/β structure.

ATP Binding and Hydrolysis. In order to determine if the expressed and purified SUR2A NBD1 S615-L933 construct is functional, we tested the ability of the protein to bind ATP using NMR spectroscopy. Although SUR2A NBD1 can be concentrated to 500 μM in the presence of MgATP, SUR2A NBD1 has limited solubility in the absence of MgATP (apo NBD1). Thus, our ATP titration experiments were done using a 50 μM apo NBD1 sample. Many of the residues in the TROSY-HSQC

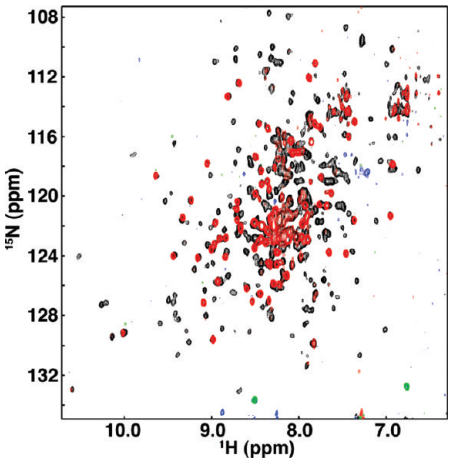

Figure 5. SUR2A NBD1 S615-L933 binds ATP. Comparison of $^{15}N-^{1}H$ TROSY HSQC spectra for 50 μM SUR2A NBD1 with and without ATP in 20 mM Na phosphate, pH 7, 150 mM NaCl, 2% (v/v) glycerol, 5 mM DTT, 10% (v/v) D_2O at 30 °C at 600 MHz. The spectrum of SUR2A NBD1 without ATP is shown in the foreground, with resonances of backbone nuclei and nuclei from side chain Trp, Asn, and Gln residues are shown in red. Aliased peaks of opposite sign, which arise from Arg side chain NεHε and backbone Gly HN correlations, are shown in green. The spectrum of SUR2A NBD1 with 2 mM Mg^{2+} and 2 mM ATP is shown in the background with resonances from backbone NH and side chain Asn, Gln, and Trp NH correlations in black. The aliased resonances of opposite sign (Arg side chain NεHε and backbone Gly HN correlations) are blue.

spectra of NBD1 in the apo state are broadened beyond detection (Figure 5), indicating dynamics on an intermediate time scale for many residues in apo NBD1. However, the presence of many strong resonances with $^{1}H^{N}$ chemical shift values >9 ppm indicate that apo NBD1 is folded, consistent with CD spectra (Figure 4D). Upon addition of ATP, many resonances reappear and the resulting spectrum overlays well with the spectrum of protein that has been purified in the presence of ATP (Figures 4A and 5), indicating that SUR2A NBD1 S615-L933 binds ATP.

We also measured the ATPase activity of isolated SUR2A NBD1 S615-L933. Similar to measurements by other groups, we obtain low rates of ATP hydrolysis for SUR2A NBD1 of ~54.0 ± 0.8 nmol Pi/mg NBD1/min that is similar to that measured for other SUR2A NBD1 constructs (31 nmol Pi/mg NBD1/min[50] and 6−9 nmol Pi/mg NBD1/min[51,52]). Differences between our values and others may be due the different boundaries used for the various constructs (S664-S884[51,52] and Q635-E889[50] compared with our optimal boundaries of S615-L933). Further, these other studies were done with the MBP fusions, rather than isolated NBDs, which may behave differently than our isolated NBD1 (S615-L933) samples in terms of ATPase activity. Differences between ATP hydrolysis rates may also be due differences in determination of protein concentration and in ATPase assays. The low ATP hydrolysis rate measured for SUR2A NBD1 S615-L933 is consistent with its monomeric behavior. Maximal ATPase activity requires NBD dimerization to form two catalytic sites, each containing the Walker A and Walker B motifs in one monomer and the signature sequence in the opposite monomer.[53] Thus, we expect to see greater ATP hydrolysis rates when NBD1 and NBD2 are included in the reaction mixture.

DISCUSSION

The generation of samples of nucleotide binding domains (NBDs) from eukaryotic ATP-binding cassette (ABC) transporters in yields that are amenable for biophysical studies such as NMR spectroscopy or X-ray crystallography has proven to be a challenging task.[16,19] Structural studies of NBD1 from CFTR, another ABCC protein, were hampered for many years because the correct boundaries were not known, and hence stable samples of the isolated protein could not be prepared.[16,19] In this paper, we demonstrate that the production of rat SUR2A NBD1 for biophysical studies can be achieved by optimizing domain boundaries that enables heterologous expression in *E. coli* of the protein in a soluble form and allows removal of a fusion partner without precipitation of the NBD. Our strategy, which combines structure-based sequence alignments, predictions of disordered regions, and biochemical and biophysical studies, has successfully produced samples of folded and functional SUR2A NBD1 for NMR spectroscopy and may be applied as general method for developing suitable constructs of other NBDs of ABC proteins.

Our structure-based sequence alignment, solubility data, and biophysical characterization indicate that SUR2A NBD1 encompasses residues S615-L933. The judicious choices for both the N- and C-terminal boundaries are factors in the production of soluble, folded, and functional SUR2A NBD1. Surprisingly, well-behaved samples of SUR2A NBD1 require extension of the C-terminal boundary to L933, which is past the C-terminal end of α-helix α9 (at D914), the last canonical secondary structure element of most NBDs. Our data comparing SUR2A NBD1 S615-L933 and S615-D914 suggest a stabilizing effect of residues Q915-L933. One possible mode for stabilization of NBD1 by the C-terminal extension, which is predicted to be disordered, may be by mediating interactions with other regions in NBD1. Although extension of the N terminus to S608 in the context of a C-terminal boundary at L933 results in a SUR2A NBD1 construct that can be produced in high yields (80 mg per liter of LB culture), the additional N-terminal residues S608-D614 may cause oligomerization and the formation of higher order aggregates in solution of the protein, similar to other NBDs. For example, the inclusion of residues N- and C-terminal to structured regions in the NBDs of P-glycoprotein leads to protein aggregation and the formation of inclusion bodies when expressed in *E. coli*.[15,54]

Deletion of residues from either the N-terminal boundary (S615) or from both the N- and C-terminal boundary (L933) affects the yield of soluble protein. Our sequence alignment and homology models indicate the β-strand β1, which is the middle β-strand of the three-stranded β-sheet subdomain, is comprised of residues S615-L623. Removal of S615-R617 in SUR2A NBD1 T618-L933 may partly destabilize the β-sheet subdomain, leading to a reduced overall yield of soluble protein. The low *in vitro* solubility of SUR2A NBD1 D665-E889 is likely attributed to removal of the entire N-terminal β-strand (β1), thus compromising folding of the entire β-sheet subdomain. The poor *in vitro* solubility of D665-E889 is likely also due additional destabilization of the protein from removal of structured regions at the C terminus, including the canonical α-helices α8 and α9, and the C-terminal extension from Q915-L933.

The identification of the N-terminal boundary of SUR2A NBD1 as S615 indicates the presence of a large insert (S627-F675) between the first two β-strands of the β-sheet subdomain in SUR2A NBD1. Seen originally for CFTR NBD1 and known as

the regulatory insert (RI) in CFTR, our alignment indicates that a β-sheet subdomain insert may be common to NBD1s of many ABCC proteins. Interestingly, there are many similarities between the β-sheet subdomain insert of SUR2A NBD1 and the RI of CFTR NBD1. Analysis of the sequence of SUR2A by PONDR indicates that much of the β-sheet subdomain insert (Q635-E664) is disordered, as seen for the CFTR RI.[16,24,44] The predicted disordered regions in SUR2A NBD1 correspond to the disordered region in CFTR RI. Further, both the SUR2A NBD1 β-sheet subdomain insert and the CFTR NBD1 RI possess a site for phosphorylation by protein kinase A (PKA). The PKA phosphorylation site in SUR2A NBD1 is at position T632 and hence is also present in SUR2C NBD1, which is missing residues Q635-K669. Thus, it is possible that there is a common mechanism by which phosphorylation of the β-sheet subdomain in SUR2A and the analogous RI in CFTR regulates these proteins. In CFTR, phosphorylation of the RI disrupts interactions of the RI and residues on the core of NBD1 that include the NBD2 dimerization surface,[43,44] leading to increased NBD1/NBD2 dimerization, ATP hydrolysis, and activation of CFTR.[55,56] Phosphorylation of T632 in SUR2A activates K_{ATP} channels,[57] possibly by allowing for enhanced NBD1/NBD2 interactions and subsequent ATP hydrolysis and opening of K_{ATP} channels. Thus, the SUR2A NBD1 β-sheet subdomain insert may also be a phosphorylation regulatory element in SUR2A that functions in a similar manner to the RI in CFTR NBD1.

The extension of the C terminus of SUR2A NBD1 beyond the canonical structured region of NBDs, which corresponds to residues C-terminal of D914 in SUR2A NBD1, may also have regulatory implications. Constructs ending at D914 contain all the canonical structured elements (i.e., to the end of α-helix α9) of NBDs. Our solubility data indicate that residues Q915-L933 impart a stabilizing effect on NBD1, possibly by mediating interactions with other regions of the protein. Such interactions may be part of a larger network of interactions that include residues D948-N942, which are involved in allosteric coupling between the activity of the NBDs and channel activation.[58] Interestingly, the NMR resonances of SUR2A NBD1 have different intensities, indicating significant dynamics that may be related to K_{ATP} channel regulation. The very intense resonances in spectra of SUR2A NBD1 centered at 8.2 ppm in the ^{1}H dimension are reflective of disorder and are likely from the β-sheet subdomain insert and the C-terminal extension. The weak resonances arise from microsecond−millisecond time scale dynamics that may involve interdomain motions important for ATP hydrolysis and/or transient interactions of the NBD core with the β-sheet subdomain and C-terminal extension. The present work, which has successfully identified boundaries of SUR2A NBD1 and generated samples of folded and functional protein for NMR studies, provides a platform for studying regulatory interactions of NBD1 to provide insights into the role of SUR2A in regulation of K_{ATP} channel activity.

■ ASSOCIATED CONTENT

Supporting Information. Supplementary Figures 1−4. This material is available free of charge via the Internet at http://pubs.acs.org.

■ AUTHOR INFORMATION

Corresponding Author

*Tel 1-905-569-4542; Fax 1-905-828-5425; e-mail voula.kanelis@utoronto.ca.

Funding Sources

This work was funded by grants from the Canadian Institutes of Health Research and the Natural Science and Engineering Council of Canada to V.K.

■ ACKNOWLEDGMENT

The authors acknowledge John L. Rubinstein and Ronald A. Venters for critically reading the manuscript and for useful discussions. The authors acknowledge Frances M. Ashcroft for providing the rat SUR2A cDNA. Amino acid analysis was done at the Advanced Protein Technology Centre at Sick Kids Hospital, Toronto, ON.

■ ABBREVIATIONS

SUR, sulfonylurea receptor; ATP, adenosine triphosphate; ABC transporter, ATP-binding cassette transporter; NBD, nucleotide binding domain; K_{ATP} channel, ATP-sensitive potassium channel; ABCC, ABC transporter C subfamily; MSD, membrane spanning domain; MRP1, multridrug resistance associated protein 1; *E. coli*, *Escherichia coli*; MBP, maltose binding protein; GST, glutathione S transferase; CD, circular dichroism; NMR, nuclear magnetic resonance; CFTR, cystic fibrosis transmembrane conductance regulator; TAP, transporter associated with antigen processing; SUMO, small ubiquitin-like modifier; IPTG, isopropyl β-D-thiogalactoside; PMSF, phenylmethylsulfonyl fluoride; SDS, sodium dodecyl sulfate; PAGE, polyacrylamide gel electrophoresis; TROSY, transverse relaxation optimized spectroscopy; HSQC, heteronuclear single quantum coherence; P*i*, inorganic phosphate; MESG, 2-amino-6-mercapto-7-methylpurine riboside; ProSA, protein structure analysis; PONDR, predictors of natural disordered regions; Ulp, ubiquitin-like protein-specific protease; RE, regulatory extension in CFTR NBD1; RI, regulatory insert in CFTR NBD1; PKA, protein kinase A.

■ REFERENCES

(1) Dean, M., Rzhetsky, A., and Allikmets, R. (2001) The human ATP-binding cassette (ABC) transporter superfamily. *Genome Res. 11*, 1156–1166.

(2) Aller, S. G., Yu, J., Ward, A., Weng, Y., Chittaboina, S., Zhuo, R., Harrell, P. M., Trinh, Y. T., Zhang, Q., Urbatsch, I. L., and Chang, G. (2009) Structure of P-glycoprotein reveals a molecular basis for poly-specific drug binding. *Science 323*, 1718–1722.

(3) Dawson, R. J., and Locher, K. P. (2006) Structure of a bacterial multidrug ABC transporter. *Nature 443*, 180–185.

(4) Ward, A., Reyes, C. L., Yu, J., Roth, C. B., and Chang, G. (2007) Flexibility in the ABC transporter MsbA: Alternating access with a twist. *Proc. Natl. Acad. Sci. U. S. A. 104*, 19005–19010.

(5) Hollenstein, K., Dawson, R. J., and Locher, K. P. (2007) Structure and mechanism of ABC transporter proteins. *Curr. Opin. Struct. Biol. 17*, 412–418.

(6) Jones, P. M., and George, A. M. (2004) The ABC transporter structure and mechanism: perspectives on recent research. *Cell. Mol. Life Sci. 61*, 682–699.

(7) Aittoniemi, J., Fotinou, C., Craig, T. J., de Wet, H., Proks, P., and Ashcroft, F. M. (2009) Review. SUR1: a unique ATP-binding cassette protein that functions as an ion channel regulator. *Philos. Trans. R. Soc., B 364*, 257–267.

(8) Mikhailov, M. V., Campbell, J. D., de Wet, H., Shimomura, K., Zadek, B., Collins, R. F., Sansom, M. S., Ford, R. C., and Ashcroft, F. M. (2005) 3-D structural and functional characterization of the purified KATP channel complex Kir6.2-SUR1. *EMBO J. 24*, 4166–4175.

(9) Zingman, L. V., Alekseev, A. E., Bienengraeber, M., Hodgson, D., Karger, A. B., Dzeja, P. P., and Terzic, A. (2001) Signaling in channel/enzyme multimers: ATPase transitions in SUR module gate ATP-sensitive K+ conductance. *Neuron 31*, 233–245.

(10) Seino, S., and Miki, T. (2003) Physiological and pathophysiological roles of ATP-sensitive K+ channels. *Prog. Biophys. Mol. Biol. 81*, 133–176.

(11) Flanagan, S. E., Clauin, S., Bellanne-Chantelot, C., de Lonlay, P., Harries, L. W., Gloyn, A. L., and Ellard, S. (2009) Update of mutations in the genes encoding the pancreatic beta-cell K(ATP) channel subunits Kir6.2 (KCNJ11) and sulfonylurea receptor 1 (ABCC8) in diabetes mellitus and hyperinsulinism. *Hum. Mutat. 30*, 170–180.

(12) Bienengraeber, M., Olson, T. M., Selivanov, V. A., Kathmann, E. C., O'Cochlain, F., Gao, F., Karger, A. B., Ballew, J. D., Hodgson, D. M., Zingman, L. V., Pang, Y. P., Alekseev, A. E., and Terzic, A. (2004) ABCC9 mutations identified in human dilated cardiomyopathy disrupt catalytic KATP channel gating. *Nature Genet. 36*, 382–387.

(13) Minoretti, P., Falcone, C., Aldeghi, A., Olivieri, V., Mori, F., Emanuele, E., Calcagnino, M., and Geroldi, D. (2006) A novel Val734Ile variant in the ABCC9 gene associated with myocardial infarction. *Clin. Chim. Acta 370*, 124–128.

(14) Olson, T. M., Alekseev, A. E., Moreau, C., Liu, X. K., Zingman, L. V., Miki, T., Seino, S., Asirvatham, S. J., Jahangir, A., and Terzic, A. (2007) KATP channel mutation confers risk for vein of Marshall adrenergic atrial fibrillation. *Nat. Clin. Pract. Cardiovasc. Med. 4*, 110–116.

(15) Booth, C. L., Pulaski, L., Gottesman, M. M., and Pastan, I. (2000) Analysis of the properties of the N-terminal nucleotide-binding domain of human P-glycoprotein. *Biochemistry (Moscow) 39*, 5518–5526.

(16) Lewis, H. A., Buchanan, S. G., Burley, S. K., Conners, K., Dickey, M., Dorwart, M., Fowler, R., Gao, X., Guggino, W. B., Hendrickson, W. A., Hunt, J. F., Kearins, M. C., Lorimer, D., Maloney, P. C., Post, K. W., Rajashankar, K. R., Rutter, M. E., Sauder, J. M., Shriver, S., Thibodeau, P. H., Thomas, P. J., Zhang, M., Zhao, X., and Emtage, S. (2004) Structure of nucleotide-binding domain 1 of the cystic fibrosis transmembrane conductance regulator. *EMBO J. 23*, 282–293.

(17) Kidd, J. F., Ramjeesingh, M., Stratford, F., Huan, L. J., and Bear, C. E. (2004) A heteromeric complex of the two nucleotide binding domains of cystic fibrosis transmembrane conductance regulator (CFTR) mediates ATPase activity. *J. Biol. Chem. 279*, 41664–41669.

(18) Neville, D. C., Rozanas, C. R., Tulk, B. M., Townsend, R. R., and Verkman, A. S. (1998) Expression and characterization of the NBD1-R domain region of CFTR: evidence for subunit-subunit interactions. *Biochemistry (Moscow) 37*, 2401–2409.

(19) Kerr, I. D., Berridge, G., Linton, K. J., Higgins, C. F., and Callaghan, R. (2003) Definition of the domain boundaries is critical to the expression of the nucleotide-binding domains of P-glycoprotein. *Eur. Biophys. J. 32*, 644–654.

(20) de Wet, H., Mikhailov, M. V., Fotinou, C., Dreger, M., Craig, T. J., Venien-Bryan, C., and Ashcroft, F. M. (2007) Studies of the ATPase activity of the ABC protein SUR1. *FEBS J. 274*, 3532–3544.

(21) Wang, C., Castro, A. F., Wilkes, D. M., and Altenberg, G. A. (1999) Expression and purification of the first nucleotide-binding domain and linker region of human multidrug resistance gene product: comparison of fusions to glutathione S-transferase, thioredoxin and maltose-binding protein. *Biochem. J. 338* (Pt 1), 77–81.

(22) Thompson, J. D., Higgins, D. G., and Gibson, T. J. (1994) CLUSTAL W: improving the sensitivity of progressive multiple sequence alignment through sequence weighting, position-specific gap penalties and weight matrix choice. *Nucleic Acids Res. 22*, 4673–4680.

(23) Larkin, M. A., Blackshields, G., Brown, N. P., Chenna, R., McGettigan, P. A., McWilliam, H., Valentin, F., Wallace, I. M., Wilm, A., Lopez, R., Thompson, J. D., Gibson, T. J., and Higgins, D. G. (2007) Clustal W and Clustal X version 2.0. *Bioinformatics 23*, 2947–2948.

(24) Lewis, H. A., Zhao, X., Wang, C., Sauder, J. M., Rooney, I., Noland, B. W., Lorimer, D., Kearins, M. C., Conners, K., Condon, B., Maloney, P. C., Guggino, W. B., Hunt, J. F., and Emtage, S. (2005) Impact of the deltaF508 mutation in first nucleotide-binding domain of human cystic fibrosis transmembrane conductance regulator on domain folding and structure. *J. Biol. Chem. 280*, 1346–1353.

(25) Gaudet, R., and Wiley, D. C. (2001) Structure of the ABC ATPase domain of human TAP1, the transporter associated with antigen processing. *EMBO J. 20*, 4964–4972.

(26) Mossessova, E., and Lima, C. D. (2000) Ulp1-SUMO crystal structure and genetic analysis reveal conserved interactions and a regulatory element essential for cell growth in yeast. *Mol. Cell 5*, 865–876.

(27) Pervushin, K., Riek, R., Wider, G., and Wuthrich, K. (1997) Attenuated T2 relaxation by mutual cancellation of dipole-dipole coupling and chemical shift anisotropy indicates an avenue to NMR structures of very large biological macromolecules in solution. *Proc. Natl. Acad. Sci. U. S. A. 94*, 12366–12371.

(28) Kanelis, V., Forman-Kay, J. D., and Kay, L. E. (2001) Multidimensional NMR methods for protein structure determination. *IUBMB Life 52*, 291–302.

(29) Delaglio, F., Grzesiek, S., Vuister, G. W., Zhu, G., Pfeifer, J., and Bax, A. (1995) NMRPipe: a multidimensional spectral processing system based on UNIX pipes. *J. Biomol. NMR 6*, 277–293.

(30) Johnson, B. A., and Blevins, R. A. (1994) NMRView: a computer program for the visualization and analysis of NMR data. *J. Biomol. NMR 4*, 603–614.

(31) Sali, A., and Blundell, T. L. (1993) Comparative protein modelling by satisfaction of spatial restraints. *J. Mol. Biol. 234*, 779–815.

(32) Sippl, M. J. (1993) Recognition of errors in three-dimensional structures of proteins. *Proteins 17*, 355–362.

(33) Wiederstein, M., and Sippl, M. J. (2007) ProSA-web: interactive web service for the recognition of errors in three-dimensional structures of proteins. *Nucleic Acids Res. 35*, W407–410.

(34) Laskowski, R. A., Rullmannn, J. A., MacArthur, M. W., Kaptein, R., and Thornton, J. M. (1996) AQUA and PROCHECK-NMR: programs for checking the quality of protein structures solved by NMR. *J. Biomol. NMR 8*, 477–486.

(35) Webb, M. R. (1992) A continuous spectrophotometric assay for inorganic phosphate and for measuring phosphate release kinetics in biological systems. *Proc. Natl. Acad. Sci. U. S. A. 89*, 4884–4887.

(36) Oswald, C., Holland, I. B., and Schmitt, L. (2006) The motor domains of ABC-transporters. What can structures tell us?. *Naunyn. Schmiedebergs Arch. Pharmacol. 372*, 385–399.

(37) Chutkow, W. A., Simon, M. C., Le Beau, M. M., and Burant, C. F. (1996) Cloning, tissue expression, and chromosomal localization of SUR2, the putative drug-binding subunit of cardiac, skeletal muscle, and vascular KATP channels. *Diabetes 45*, 1439–1445.

(38) Li, X., Romero, P., Rani, M., Dunker, A. K., and Obradovic, Z. (1999) Predicting Protein Disorder for N-, C-, and Internal Regions. *Genome Inform. Ser. Workshop Genome Inform. 10*, 30–40.

(39) Romero, O., and Dunker, K. (1997) Sequence Data Analysis for Long Disordered Regions Prediction in the Calcineurin Family, *Genome Inform. Ser. Workshop Genome Inform. 8*, 110–124.

(40) Romero, P., Obradovic, Z., Li, X., Garner, E. C., Brown, C. J., and Dunker, A. K. (2001) Sequence complexity of disordered protein. *Proteins 42*, 38–48.

(41) Park, S., Lim, B. B., Perez-Terzic, C., Mer, G., and Terzic, A. (2008) Interaction of asymmetric ABCC9-encoded nucleotide binding domains determines KATP channel SUR2A catalytic activity. *J. Proteome Res. 7*, 1721–1728.

(42) Park, S., and Terzic, A. (2010) Quaternary structure of KATP channel SUR2A nucleotide binding domains resolved by synchrotron radiation X-ray scattering. *J. Struct. Biol. 169*, 243–251.

(43) Baker, J. M., Hudson, R. P., Kanelis, V., Choy, W. Y., Thibodeau, P. H., Thomas, P. J., and Forman-Kay, J. D. (2007) CFTR regulatory region interacts with NBD1 predominantly via multiple transient helices. *Nat. Struct. Mol. Biol. 14*, 738–745.

(44) Kanelis, V., Hudson, R. P., Thibodeau, P. H., Thomas, P. J., and Forman-Kay, J. D. (2010) NMR evidence for differential phosphorylation-dependent interactions in WT and DeltaF508 CFTR. *EMBO J. 29*, 263–277.

(45) Obradovic, Z., Peng, K., Vucetic, S., Radivojac, P., and Dunker, A. K. (2005) Exploiting heterogeneous sequence properties improves prediction of protein disorder. *Proteins 61* (Suppl. 7), 176–182.

(46) Yuan, Y. R., Blecker, S., Martsinkevich, O., Millen, L., Thomas, P. J., and Hunt, J. F. (2001) The crystal structure of the MJ0796 ATP-binding cassette. Implications for the structural consequences of ATP hydrolysis in the active site of an ABC transporter. *J. Biol. Chem. 276*, 32313–32321.

(47) Malakhov, M. P., Mattern, M. R., Malakhova, O. A., Drinker, M., Weeks, S. D., and Butt, T. R. (2004) SUMO fusions and SUMO-specific protease for efficient expression and purification of proteins. *J. Struct. Funct. Genomics 5*, 75–86.

(48) Sanchez-Puig, N., Veprintsev, D. B., and Fersht, A. R. (2005) Human full-length Securin is a natively unfolded protein. *Protein Sci. 14*, 1410–1418.

(49) Ramaen, O., Leulliot, N., Sizun, C., Ulryck, N., Pamlard, O., Lallemand, J. Y., Tilbeurgh, H., and Jacquet, E. (2006) Structure of the human multidrug resistance protein 1 nucleotide binding domain 1 bound to Mg2+/ATP reveals a non-productive catalytic site. *J. Mol. Biol. 359*, 940–949.

(50) de Wet, H., Fotinou, C., Amad, N., Dreger, M., and Ashcroft, F. M. (2010) The ATPase activities of sulfonylurea receptor 2A and sulfonylurea receptor 2B are influenced by the C-terminal 42 amino acids. *FEBS J. 277*, 2654–2662.

(51) Bienengraeber, M., Alekseev, A. E., Abraham, M. R., Carrasco, A. J., Moreau, C., Vivaudou, M., Dzeja, P. P., and Terzic, A. (2000) ATPase activity of the sulfonylurea receptor: a catalytic function for the KATP channel complex. *FASEB J. 14*, 1943–1952.

(52) Masia, R., Enkvetchakul, D., and Nichols, C. G. (2005) Differential nucleotide regulation of KATP channels by SUR1 and SUR2A. *J. Mol. Cell. Cardiol. 39*, 491–501.

(53) Smith, P. C., Karpowich, N., Millen, L., Moody, J. E., Rosen, J., Thomas, P. J., and Hunt, J. F. (2002) ATP binding to the motor domain from an ABC transporter drives formation of a nucleotide sandwich dimer. *Mol. Cell 10*, 139–149.

(54) Dayan, G., Jault, J. M., Baubichon-Cortay, H., Baggetto, L. G., Renoir, J. M., Baulieu, E. E., Gros, P., and Di Pietro, A. (1997) Binding of steroid modulators to recombinant cytosolic domain from mouse P-glycoprotein in close proximity to the ATP site. *Biochemistry (Moscow) 36*, 15208–15215.

(55) Csanady, L., Chan, K. W., Seto-Young, D., Kopsco, D. C., Nairn, A. C., and Gadsby, D. C. (2000) Severed channels probe regulation of gating of cystic fibrosis transmembrane conductance regulator by its cytoplasmic domains. *J. Gen. Physiol. 116*, 477–500.

(56) Li, C., Ramjeesingh, M., Wang, W., Garami, E., Hewryk, M., Lee, D., Rommens, J. M., Galley, K., and Bear, C. E. (1996) ATPase activity of the cystic fibrosis transmembrane conductance regulator. *J. Biol. Chem. 271*, 28463–28468.

(57) Quinn, K. V., Giblin, J. P., and Tinker, A. (2004) Multisite phosphorylation mechanism for protein kinase A activation of the smooth muscle ATP-sensitive K+ channel. *Circ. Res. 94*, 1359–1366.

(58) Karger, A. B., Park, S., Reyes, S., Bienengraeber, M., Dyer, R. B., Terzic, A., and Alekseev, A. E. (2008) Role for SUR2A ED domain in allosteric coupling within the K(ATP) channel complex. *J. Gen. Physiol. 131*, 185–196.